



Wiesław Frącz\*, Grzegorz Janowski, Grażyna Rzyńska

Rzeszów University of Technology, Department of Materials Forming and Processing, al. Powstańców Warszawy 8, 35-959 Rzeszów, Poland  
\*Corresponding author. E-mail: wf@prz.edu.pl

Received (Otrzymano) 26.04.2017

## STRENGTH ANALYSIS OF GFRP COMPOSITE PRODUCT TAKING INTO ACCOUNT ITS HETEROGENIC STRUCTURE FOR DIFFERENT REINFORCEMENTS

In this study prediction of the strength properties of composites made of polyester resin and continuous glass fiber reinforcement in established grades was performed. Structure modeling based on the numerical homogenization method was conducted using Digimat FE commercial code, taking into account the geometry and properties of all the composite components. In the first stage, analysis was performed for OCF M8610 mat. At the beginning the calculations were done for beam roving from S glass. Preliminary calculations were performed for the virtual composition of glass fibers-air, which allowed calculation of the yarn properties, directly used to build the glass mat model. The second stage of the calculation was carried out for glass mat saturated with polyester resin. For this purpose, roving bundle data and polymer matrix data were implemented. The volume fraction of the glass mat in the composite was also determined, and a random fiber orientation in the plane was defined. The properties of the fabric-resin composite were calculated for polyester resin and Cofab A1118B glass fiber plain weave fabric. The basic properties of the fiber in the analyzed bi-directional fabric were established on the basis of literature. The calculation of some fabric properties was conducted by a different algorithm than in the case of the mat. The last stage of property calculation for the warp and weft was to predict the weave properties based on the manufacturer's data. Only at this stage was the mean field method (MFM) used in the calculations. The geometrical dimensions of the reinforcements were calculated including its grammage, where the value is highly compatible with the grammage given in the literature. For both types of reinforcement visualization of the composite structure was performed. The calculated composite properties were used in strength simulations of a useful product for three variants of composite reinforcement: (a) polyester resin without reinforcement, (b) polyester resin with glass fiber mat, (c) polyester resin with glass fiber fabric, which allowed carrying out a comparative strength analysis.

Keywords: GFRP composites, numerical homogenization, Digimat software

## ANALIZA WYTRZYMAŁOŚCIOWA WYROBU Z KOMPOZYTU GFRP Z UWZGLĘDNIENIEM JEGO HETEROGENICZNEJ STRUKTURY DLA RÓŻNEGO ZBROJENIA

W pracy przeprowadzono prognozowanie wytrzymałości kompozytów wykonanych z żywicy poliestrowej i tkaniny lub maty z włókien szklanych w ustalonych gatunkach. Modelowanie struktury kompozytów wykonano z wykorzystaniem metody numerycznej homogenizacji z użyciem oprogramowania Digimat FE, biorąc pod uwagę geometrię i właściwości każdego składnika kompozytu. W pierwszym etapie przeprowadzono analizę dla maty w gatunku OCF M8610. Wykonano niezbędne obliczenia dla jednej wiązki rowingu typu S. Wstępne obliczenia dotyczyły wariantu kompozycji: włókna szklane - powietrze. Umożliwiły one obliczenie właściwości przędzy, bezpośrednio wykorzystywanej do budowy modelu maty szklanej. W drugim etapie przeprowadzono obliczenia dla kompozycji: mata - żywica poliestrowa. W tym celu uwzględniono dane wiązki i osnowy polimerowej. Określono także udział objętościowy maty szklanej w kompozycie oraz zdefiniowano, jako losową, orientację włókien w płaszczyźnie. Właściwości kompozycji typu tkanina - żywica obliczono dla tkaniny z włókna szklanego w gatunku Cofab A1118B i żywicy poliestrowej. Podstawowe właściwości włókna w analizowanej dwukierunkowej tkaninie zostały ustalone na podstawie literatury. Obliczenie niektórych właściwości tkaniny wykonano za pomocą innego algorytmu niż w przypadku maty. Ostatnim etapem obliczania właściwości osnowy i wątku było określenie splotu tkaniny zgodnie z danymi producenta. Obliczono geometryczne wymiary wzmocnienia kompozytu, w tym jego gramaturę, której wartość w dużym stopniu jest zgodna z gramaturą tkaniny określoną przez producenta. Wyłącznie na tym etapie zastosowano w kalkulacjach metodę homogenizacji uśrednionego pola (ang. MFM). Dla obydwóch typów wzmocnienia wykonano wizualizację struktury kompozytów. Obliczone właściwości kompozytu zostały wykorzystane do symulacji wytrzymałości wytworu użytkowego dla trzech wariantów wzmocnienia: a) żywicy poliestrowej bez zbrojenia, b) żywicy poliestrowej z matą z włókna szklanego, c) żywicy poliestrowej z tkaniną z włókna szklanego, co pozwoliło na przeprowadzenie wytrzymałościowej analizy porównawczej.

Słowa kluczowe: kompozyty GFRP, homogenizacja numeryczna, program Digimat

## INTRODUCTION AND AIM OF STUDY

The properties of the composite materials on the macro scale are strongly dependent on the properties of the composite components. The properties of inclusions (reinforcement) are not always separately considered,

and therefore the averaging procedure is used. Defining the macroscopic properties of a material is done by homogenization methods to extract the characteristics of a representative material area with inclusions (composite components) and averaging it to the macro scale. The main purpose of homogenization methods is to obtain relevant data describing the material model that can represent the all the macroscopic properties and heterogeneous composite structure. For many years homogenization methods were developed by means of analytical models that did not always provide calculation accurate results. This is due to, among others, newly created material compositions with specific properties for which these models do not allow one to adequately obtain a detailed description of their micro-structure [1-3].

**Governing equations**

Considering a heterogeneous composite with periodic structures, it consists of at least two components (Fig. 1). Composites have two length scales: a global length scale that is of the order of the body size, and a local length scale that is proportionate to the wavelength of the variation of the micro-structure. The dimensions of the reinforced body (unit cell) were assumed to be much smaller than the size of the body.

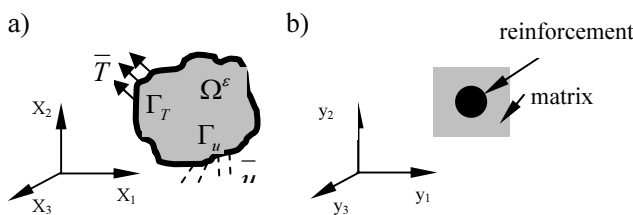


Fig. 1. Elastic composite model  $\Omega^\epsilon$  (a), representative unit cell  $Y$  (b)

Rys. 1. Model kompozytu o właściwościach sprężystych  $\Omega^\epsilon$  (a), komórka reprezentatywna (b)

The relation between global coordinate system  $x_i$  of the whole composite and local system  $y_i$  for the unit cell can be written as

$$y_i = \frac{x_i}{\epsilon} \tag{1}$$

where:  $\epsilon$  - the scale factor between the two length scales.

For a real heterogeneous composite, when it is subjected to external forces, field quantities such as displacement and stress will vary with global coordinate system  $x$ . The field quantities will vary rapidly within the neighborhood of  $\epsilon$  within a short wavelength because of the nonlinearity of the microstructure. The unknown strain ( $e_{ij}$ ), displacement ( $u_i$ ) and stress ( $\sigma_{ij}$ ), are calculated on the basis of the physical equation, geometric equation and equilibrium equation:

$$e_{ij}^\epsilon = \frac{1}{2}(u_{i,j}^\epsilon + u_{j,i}^\epsilon) \text{ in } \Omega^\phi, \tag{2}$$

$$\sigma_{ij}^\epsilon = C_{ijkl}^\epsilon e_{kl}^\epsilon \text{ in } \Omega^\phi \tag{3}$$

$$\sigma_{ij,j}^\epsilon + f_i = 0 \text{ in } \Omega^\phi, \tag{4}$$

and boundary conditions:

$$u_i^\epsilon = \bar{u}_i \text{ on } \Gamma_u^\epsilon \tag{5}$$

$$\sigma_{ij}^\epsilon n_j = \bar{T}_i \text{ on } \Gamma_T^\epsilon, \tag{6}$$

where  $C_{ijkl}$  is the composite stiffness matrix,  $f_i$  is the body force,  $n_j$  is the outward normal vector of the boundary,  $T_i$  is the given external force on boundary  $\Gamma_T^\epsilon$  and  $\bar{u}_i$  is the given displacement on boundary  $\Gamma_U^\epsilon$ .

These relationships describe the conditions for the exemplary representative volume element (RVE), which contains all the information needed for complete description of the structure and properties for the whole material [4-7].

**SCOPE OF WORK**

Attempts are currently being made to develop methods of homogenization which allow visualization of the 3D structure model of inclusions in the matrix as well. This makes it possible to obtain accurate results compared with analytical methods. They may greatly reduce the number of expensive and time-consuming experiments aimed at predicting the properties of the material. To take into account the actual number of inclusions in the whole material, generating a structure model with a very fine mesh of finite elements (FE) of a size smaller than the FE inclusions is required, which makes the calculation virtually impossible to achieve even for the capabilities of contemporary computers. In that case RVE are used. In principle, the RVE represents the whole material by volume with a finite amount of inclusions reflecting the behavior at the micro level, allowing easy discretization of this area and enabling the performance of numerical calculations [8, 9].

In the range of tests microstructural analyses were performed for fiber composites with polyester resin, taking into account two reinforcement variants: glass fiber mats and fabrics, to determine the properties of the composites with regard to their heterogeneous structure. The necessary properties of composite components for numerical analysis were determined based on the literature [8-17]. All the calculations of the composite properties were performed using Digimat FE commercial code [18]. This software allows one to take into account the heterogeneous properties of composites by, among others, homogenization numerical methods. The size of the specified RVE was selected to include the greatest possible amount of reinforcement, whose geometrical

models were discretized by finite elements (FE) of sizes ten times smaller than the smallest dimension of the inclusions (component). This gave the opportunity, in terms of computing capability, to perform a precise analysis. The results were used in strength simulations of a useful product, which enabled comparative analysis of the composites.

## CALCULATION OF VARIANTS FOR POLYESTER RESIN - GLASS FIBRE COMPOSITES

### Variant I - stage I

In the first stage, analysis was performed for OCF M8610 mats [9-12, 16]. First phase calculations were done for beam roving (thickness of 140  $\mu\text{m}$ ) from S glass fiber (Table 1). An RVE size of 0.075 x 0.075 x 0.075 mm was assumed in the calculations, taking into account parallel arrangement of the roving fibers (Fig. 2). Preliminary calculations were performed for the composition of glass fiber-air (glass fiber mass content was 99.9848%), which allowed calculation of the yarn properties (Table 2), directly used to build the glass mat model.

TABLE 1. Properties of S-glass fiber used in calculations  
TABELA 1. Właściwości włókna szklanego typu S uwzględnione w obliczeniach

Fiber diameter	15 $\mu\text{m}$
Density	2490 $\text{kg}/\text{m}^3$
Young's modulus	85500 MPa
Poisson's coefficient	0.22

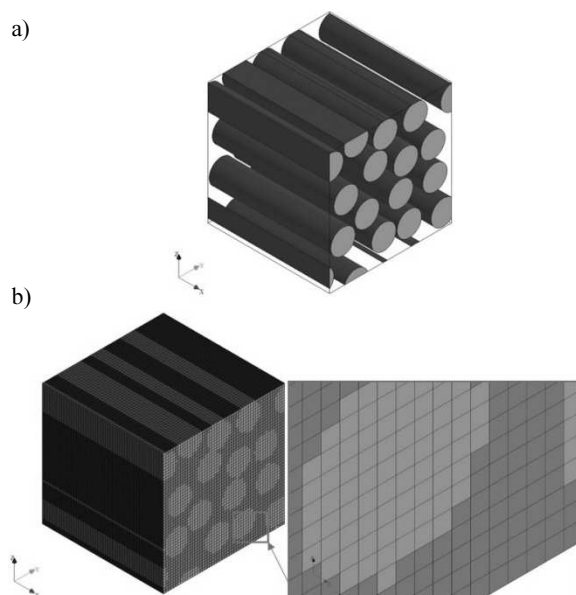


Fig. 2 Visualization for mats: a) location of fibers in RVE, b) RVE after discretization of 125 000 Voxel FE (Voxel size for single cell 0.0015x0.0015x0.0015 mm)

Rys. 2. Wizualizacja dla maty: a) układ włókien w RVE, b) RVE po dyskretyzacji za pomocą 125 tys. ES typu Voxel (rozmiar pojedynczego Voxela 0,0015x0,0015x0,0015 mm)

TABLE 2. Mechanical properties of beam roving calculated by means of Digimat FE

TABELA 2. Właściwości pojedynczej wiązki rovingu obliczone za pomocą Digimat FE

Density	1892,6912 $\text{kg}/\text{m}^3$
Young's modulus E1	130834 MPa
Young's modulus E2	123067 MPa
Poisson's coefficient $\nu_{12}$	0.2699
Poisson's coefficient $\nu_{21}$	0.2539
Kirchhoff's modulus	47407 MPa

### Variant I - stage II

Then the second stage of the calculation for the glass mat saturated with polyester resin was carried out. For this purpose, roving bundle data (obtained from a prior analysis) and polymer matrix data were implemented (Table 3). The beam diameter of yarn equal to 140  $\mu\text{m}$  was assumed as the mean value [10]. The volume fraction of the glass mat in the composite was also determined (11.97%), and a random fiber orientation in the plane (orientation type in Digimat: Random 2D) was defined. Based on the geometric data of glass mat, the representative RVE with dimensions of 1.8 x 1.8 x 1.8 mm was generated (Fig. 3), which was discretized by 2 125 364 voxel type FE (size of a single voxel: 0.014x0.014x0.014 mm) and then the calculations of composite properties were made, whose results are summarized in Table 4.

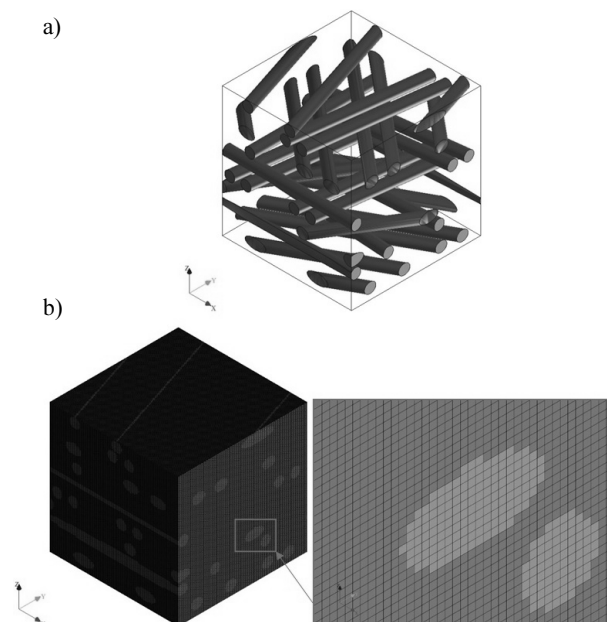


Fig. 3. Visualization of yarn: a) orientation of glass mat saturated with polyester resin, b) RVE glass mat with polymer matrix after discretization

Rys. 3. Wizualizacja orientacji przędzy: a) dla maty szklanej przesyconej żywicą poliestrową, b) RVE maty szklanej z matrycą polimerową po dyskretyzacji

TABLE 3. Properties of polyester resin  
TABELA 3. Właściwości żywicy poliestrowej

Density	1200 kg/m <sup>3</sup>
Young's modulus	4000 MPa
Poisson's coefficient	0.4

TABLE 4. Properties for calculated composition: glass mat-polyester resin

TABELA 4. Właściwości otrzymanej kompozycji: mata szklana - żywica poliestrowa

Density	1282.8301 kg/m <sup>3</sup>
Young's modulus E1	9745.8903 MPa
Young's modulus E2	9568.1602 MPa
Young's modulus E3	6586.1202 MPa
Poisson's coefficient $\nu_{12}$	0.3298
Poisson's coefficient $\nu_{21}$	0.3238
Poisson's coefficient $\nu_{13}$	0.4174
Poisson's coefficient $\nu_{31}$	0.2821
Poisson's coefficient $\nu_{23}$	0.4231
Poisson's coefficient $\nu_{32}$	0.2913
Kirchhoff's modulus G12	3059.6410 MPa
Kirchhoff's modulus G23	1857.9101 MPa
Kirchhoff's modulus G13	1849.6112 MPa

#### Variant II - calculations for composite: fabric-resin

The properties of the fabric-resin composite were calculated for the polyester resin-glass fiber fabric. The basic properties of the fiber in the analyzed Cofab A1118Bbi-directional fabrics (plain weave) were established on the basis of literature (Table 5) [13-17]. Calculation of the fabric properties was made by a different algorithm than in the case of the mat. First the geometrical data of the warp and weft were defined (Table 6), which allowed carrying out the preliminary calculations. It should be noted that only at this stage was the averaged field homogenization method (called MFM) used in the calculations. The calculated properties of the warp and weft are presented in Table 7.

TABLE 5. Properties of E-glass fiber used in calculation

TABELA 5. Właściwości włókna szklanego typu E

Fiber diameter	9 $\mu$ m
Density	2560 kg/m <sup>3</sup>
Young's modulus	72000 MPa
Poisson's coefficient	0.22

TABLE 6. Parameters of warp and weft for resin-fabric composition

TABELA 6. Parametry wątku i osnowy dla kompozycji żywica - tkanina

Linear density of yarn	1102 tex (g/km)
Warp height	0.48 mm
Warp width	2.5 mm
Weft height	0.48 mm
Weft width	2.7 mm

TABLE 7. Mechanical properties of warp and weft for Cofab A1118B calculated by Digimat

TABELA 7. Właściwości mechaniczne wątku oraz osnowy dla Cofab A1118B obliczone za pomocą Digimat

	Weft	Warp
Young's modulus E1	35162 MPa	32854 MPa
Young's modulus E2	11475 MPa	10498 MPa
Poisson's coefficient $\nu_{12}$	0.5238	0.5320
Poisson's coefficient $\nu_{21}$	0.2999	0.3073
Kirchhoff's modulus	4141.3 MPa	3746.3 MPa

The last stage of property calculation for the warp and weft was to predict the weave properties on the basis of the manufacturer's data. The geometrical dimensions of the reinforcements (Table 8) was calculated including its grammage, where the value is highly compatible with the grammage given in the literature [13]. The relative error between the real (on the basis of producer technical data) and calculated grammage value (610 g/m<sup>2</sup>) was 2.8%, which confirms the correctness of the calculation method and the accuracy of the mechanical data.

TABLE 8. RVE technical data for Cofab A1118B fabric

TABELA 8. Dane techniczne tkaniny Cofab A1118B

RVE dimensions	7.4074 mm x 7.60456 mm x 0.96 mm
Fabric grammage	592.8381 g/m <sup>2</sup>
Fiber volume fraction	0.2412

In next stage the dimensions of the RVE for the fabric-polymer resin composite were determined (Fig. 4). The RVE was discretized by means of 493 865 voxel FE (dimension of a single voxel: 0.048x0.048x0.048 mm). The results of the calculations were analyzed and presented in Table 9.

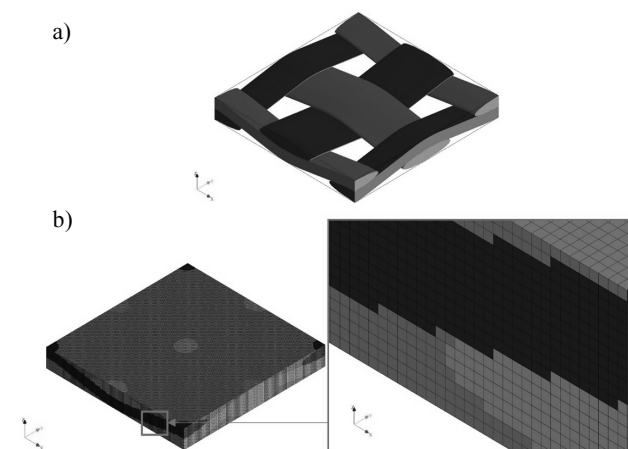


Fig. 4. Visualization of fabric: a) fabric wave, b) RVE after discretization

Rys. 4. Wizualizacja obszaru tkaniny: a) splot tkaniny przesyconej żywicą, b) RVE po dyskretyzacji

TABLE 9. Calculated properties of fabric-polyester resin composition

TABELA 9. Właściwości otrzymanej kompozycji tkanina - żywica poliestrowa

Density	1947.3811 kg/m <sup>3</sup>
Young's modulus E1	13217.4002 MPa
Young's modulus E2	13508.7023 MPa
Young's modulus E3	8057.5901 MPa
Poisson's coefficient v12	0.1991
Poisson's coefficient v21	0.2035
Poisson's coefficient v13	0.4724
Poisson's coefficient v31	0.2879
Poisson's coefficient v23	0.4674
Poisson's coefficient v32	0.2788
Kirchhoff's coefficient G12	2546.9611 MPa
Kirchhoff's modulus G23	2328.1101 MPa
Kirchhoff's modulus G13	2341.9712 MPa

## STRENGTH ANALYSIS OF PRODUCT FOR REINFORCEMENT VARIANTS

The results of property calculations for heterogeneous composites make it possible to perform advanced numerical analyzes, taking into account the behavior of products made of composites under loads. For this purpose, load simulations of a car seat used as equipment in public transport vehicles were conducted. Numerical analysis was performed for three variants of reinforcement: a) polyester resin without reinforcement, b) polyester resin with glass fiber mat, and c) polyester resin with glass fiber fabric. During the simulations, due to computational difficulties related to the composite model, only a single reinforcement layer was taken into account. The thickness of the real fabric layer was 0.96 mm. The thickness of the real mats layer was 1.5 mm. The geometric model of the seat (610 x 458 x 565 mm, thickness of 3 mm) was designed by means of NX9 software. It was assumed that the seat would be equipped with a metal connector attached to the vehicle floor by means four screws. The complete seat model was imported to Ansys ver. 14.5 commercial code to carry out behavior numerical analysis under load. The analysis was performed in terms of static loads. The boundary conditions (Fig. 5), i.e. the load assumed by the seat surface ( $F_1 = 1000$  N) and the force acting on the bearing surface ( $F_2 = 300$  N) were introduced. Between the bottom of the car seat and the upper surface of the metal connector a displacement of 0.5 mm was allowed, which represented the clearance resulting from the assembly of components (the seat and the connector) using screws. The lower surface of the connector was fixed. The next step was to introduce the

composite properties for the three reinforcements variants to the software. Due to the anisotropic properties of the mats and fabrics, calculations by means of the Ansys code were carried out in the local coordinate systems of the seat and backrest. They were carried out in order to take into account the material properties of properly oriented reinforcement. It was assumed that the screws and connector were made of steel.

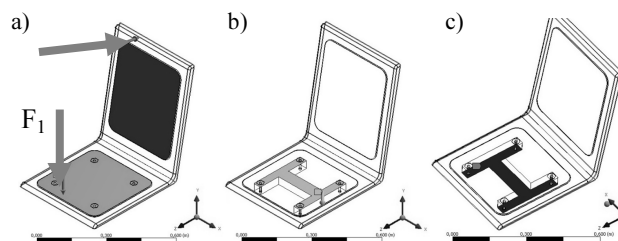


Fig. 5. Boundary conditions and loads: a) forces applied to seat surface and backrest, b) fixed displacement between lower seat surface, and connector, c) lower restraint surface

Rys. 5. Warunki brzegowe i obciążenie fotela: a) powierzchnia przyłożenia obciążenia do siedziska fotela oraz do oparcia, b) obszar założonego przemieszczenia między dolną powierzchnią fotela a metalowym łącznikiem, c) utwierdzenie dolnej powierzchni

In the performed simulations of seat load, the comparison criterion was the maximum deflection of the backrest. As shown in Figure 6 the greatest amount of deflection was found, which is evident, in the case of the resin without reinforcement.

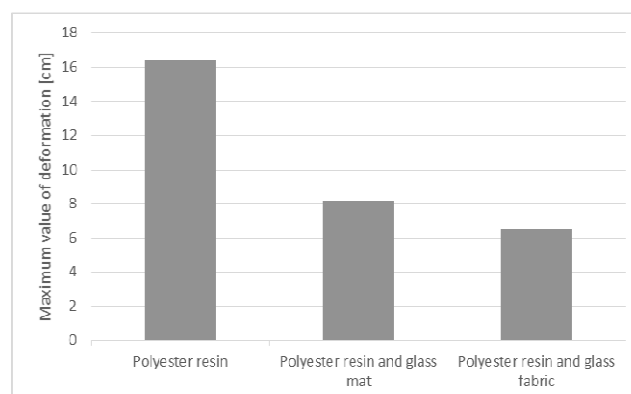


Fig. 6. Maximum deflection of seat backrest for three composite variants

Rys. 6. Maksymalne ugięcie oparcia fotela dla wariantów kompozytu

For the composites reinforced by mat and fabric, deflections of 80 and 60 mm were obtained. Analysis was performed for the composite without a metal frame, which is rarely used in the construction of such seats. By analysing the results, it can be noted that in the case of glass fiber fabric the value of backrest deflection can be reduced several times. The use of glass fiber reinforcement significantly improves composite stiffness (Fig. 7), and therefore reduces the thickness and weight of the analyzed composite seat.

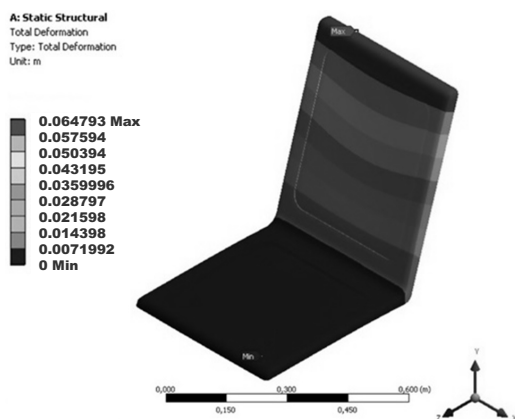


Fig. 7. Total deformation of seat made of composite: polyester resin-glass fabric

Rys. 7. Odształcenia fotela dla wariantu kompozytu: żywica poliestro-wa - tkanina szklana

## CONCLUSIONS

The use of numerical homogenization methods during strength calculations by means of Digimat FE commercial code allows one to take into account the actual geometry data and properties of components in a composite structure.

Two-step calculations for glass mat saturated with the required resin must be performed: one for single beam roving and subsequently for the representative area of mats saturated with resin. In the case of plain weave fabrics, the first calculations should be made for the thread and the warp and then the calculations are carried out for the representative area of fabric.

Appropriate sizing of RVE and voxel FE mesh allow one to receive very high compliance between the results of the calculated grammage and literature data. This proves the high effectiveness of the numerical homogenization method used in structure modeling.

The results of load simulation for the model of passenger seat (for two types of composite: with and without reinforcement) show that the use of reinforcement significantly affects a reduction in the maximum seat backrest deflection. In the case of glass fiber fabric reinforcement, the deflection can be reduced up to approx. 100% percent compared with a product made without reinforcement. The smallest deformation of the product was obtained for the composite with reinforced fabric. These deformations are approx. 25% less than for the mat.

The Digimat FE commercial code enables visualization of the real composite structure as well.

## Acknowledgement

*The research leading to these results received funding from the People's Programme (Marie Curie International Research Staff Exchange) of the European Union's Seventh Framework Programme FP7/2007-2013/ under REA grant agreement PIRSES-GA-2013-610547.*

## REFERENCES

- [1] Fliegner S., Micromechanical finite element modeling of long fiber reinforced thermoplastics (doctoral dissertation, Ph.D. thesis), Karlsruhe Institute of Technology (KIT), 2015.
- [2] Doghri I., El Ghezal M.I., Adam L., Finite strain mean-field homogenization of composite materials with hyperelastic-plastic constituents, *International Journal of Plasticity* 2016, 81, 40-62.
- [3] Doghri I., Ouair A., Homogenization of two-phase elasto-plastic composite materials and structures: study of tangent operators, cyclic plasticity and numerical algorithms, *International Journal of Solids and Structures* 2003, 40, 1681-1712.
- [4] Sun, Huiyu, et al., Micromechanics of composite materials using multivariable finite element method and homogenization theory, *International Journal of Solids and Structures* 2001, 38.17, 3007-3020.
- [5] Sun C.T., Vaidya R.S., Prediction of composite properties from a representative volume element, *Composites Science and Technology* 1996, 56.2, 171-179.
- [6] Karihaloo B.L., Xiao Q.Z., Wu C.C., Homogenization-based multivariable element method for pure torsion of composite shafts, *Computers & Structures* 2001, 79.18, 1645-1660.
- [7] Frącz W., Janowski G., Strength analysis of molded pieces produced from wood-polymer composites (WPC) including their complex structures, *Composites Theory and Practice* 2016, 16, 260-265.
- [8] Al Kassem G., Weichert D., Micromechanical material models for polymer composites through advanced numerical simulation techniques, *PAMM*, 9, 413-414.
- [9] Pierard O., Llorca J., Segurado J., Doghri I. (2007), Micromechanics of particle-reinforced elasto-viscoplastic composites: finite element simulations versus affine homogenization, *International Journal of Plasticity* 2009, 23, 1041-1060.
- [10] Kim D.S., Macosko C.W., Reaction injection molding process of glass fiber reinforced polyurethane composites, *Polymer Engineering & Science* 2000, 40(10), 2205-2216.
- [11] Dominguez R.J., Rice D.M., High strength continuous glass strand-polyurethane composites by the reaction injection molding process, *Polymer Composites* 1983, 4, 185-189.
- [12] Hedley C.W., Mold filling parameters in resin transfer molding of composites (doctoral dissertation), Montana State University Bozeman, 1994.
- [13] Trevino L., Rupel K., Young W.B., Liou M.J., Lee L.J., Analysis of resin injection molding in molds with preplaced fiber mats. I: Permeability and compressibility measurements, *Polymer Composites* 1991, 12, 20-29.
- [14] Yu B., James Lee L., A simplified in-plane permeability model for textile fabrics, *Polymer Composites* 2000, 21, 6605.
- [15] Yu B.M., Li J.H., Zhang D.M., A fractal trans-plane permeability model for textile fabrics, *International Communications in Heat and Mass Transfer* 2003, 30, 127-138.
- [16] Batch G.L., Cumiskey S., Macosko C.W., Compaction of fiber reinforcements, *Polymer Composites* 2002, 23, 307-318.
- [17] Material database from Autodesk Moldflow Insight 2013 commercial code.
- [18] DIGIMAT software documentation, e-Xstream engineering, 2015.